$u=(3-s)/2s$. A preprint[8] of their work has recently appeared and a portion of it applied to this type-IX metric. Their qualitative picture of the solution and ours are consistent, and they provide a corresponding numerical example; however, their techniques are entirely different [they make no use of the Lagrangian (7) nor the potential (8)], and they do not consider the significance of the results for the questions of horizons and the establishment of large scale homogeniety in the early universe.

The Lifshitz-Khalatnikov[8] bounce law

$$B: u \to u-1 \qquad (14)$$

is much easier to use than B_3 above. The two are related by $B=P_{23}B_3P_{12}P_{13}$, where the P's are operators permuting the Kasner exponents p_1, p_2, p_3 namely $P_{23}: u \to 1/u$, $P_{12}: u \to -(1+u)$, and $P_{13}: u \to -u/(1+u)$. It appears that almost all solutions come arbitrarily close to the values $u=-1, 0, \infty$ $(s=-3, +3, 0)$ which we recognize as the states giving communication along the three corresponding expansion axes of the universe. To see this, start with $u>1$ by using the permutations to put u in the standard interval $u \geqslant 1$ (one of the six permutation-equivalent intervals with end points $u=-\infty, -2, -1, -\frac{1}{2}, 0, 1, \infty$). Then after a finite number of steps $u \to u-1$, which correspond to $\beta(\Omega)$ rattling back and forth between the walls leading to one fixed corner of the potential, one will find $0 \leqslant u \leqslant 1$. The permutation $u \to 1/u$ then resets $u \geqslant 1$ again, to let β begin rattling in another corner. On the basis of this analysis, a countable set of initial u values could avoid $u=0$ by a finite amount; these would be fixed points of operators $P_{12}B^{n_1}P_{12}B^{n_2}P_{12}\cdots B^{n_k}$. The simplest of these is $P_{12}B$ with fixed point $u_f=\frac{1}{2}(1+5^{1/2})$, for which β bounces off every wall of the triangular potential in turn without ever heading toward a corner. This behavior is unstable, however, and some of the exponentially small terms neglected in Eq. (9) when deriving (14) will no doubt divert the corresponding exact solutions toward the $u \to 0$ stages which open up horizon limits.

A full account of this work will be submitted for publication elsewhere.

---

*Research supported in part by National Aeronautics and Space Administration Grant No. NSG-21-002-010.

[1]W. Rindler, Monthly Notices Roy. Astron. Soc. 116, 6 (1956).

[2]For references and a brief review see S. W. Hawking and G. F. R. Ellis, Astrophys. J. 152, 25 (1968), Secs. V, VI; and O. Heckmann and E. Schucking, in Gravitation: An Introduction to Current Research, edited by L. Witten (John Wiley & Sons, Inc., New York, 1962), Chap. II.

[3]See, e.g., E. M. Lifshitz and I. M. Khalatnikov, Advan. Phys. 12, 185 (1963).

[4]S. W. Hawking, Adams Prize Essay, Cambridge University, 1966 (unpublished).

[5]Similar techniques have been used for a type-I metric: C. W. Misner, Astrophys. J. 151, 431 (1968).

[6]C. W. Misner and A. H. Taub, Zh. Eksperim. i Teor. Fiz. 55, 233 (1968).

[7]J. A. Wheeler, private communication.

[8]V. A. Belinski and I. M. Khalatnikov, to be published. I thank Professor K. S. Thorne for making this preprint available to me in an English translation by Dr. A. Pogo.

OMEGA AND ETA PRODUCTION IN $\pi^+d \to pp\pi^+\pi^-\pi^0$ AT 3.65 BeV/c *

G. C. Benson,† B. P. Roe, D. Sinclair, and J. C. Vander Velde
The University of Michigan, Ann Arbor, Michigan 48104
(Received 28 February 1969)

We have observed ~3000 examples of the reaction $\pi^+d \to pp\pi^+\pi^-\pi^0$ and report on ~300 events in which the $\pi^+\pi^-\pi^0$ mass is in the ω^0 mass region and ~40 events in the η^0 mass region. Differential cross sections are presented. There is evidence for a backward peak in the overall channel. We give values for the ω^0 density-matrix elements in the forward direction. Our value for Reρ_{10} is negative, in disagreement with various theoretical models.

In an exposure of 3.65-BeV/c π^+ in the Brookhaven National Laboratory 20-in. bubble chamber we have observed ~3000 examples of the reaction $\pi^+d \to p_S p\pi^+\pi^-\pi^0$. We report here on an analysis of those events in which the $\pi^+\pi^-\pi^0$ invariant mass is in the ω^0 or η^0 regions, giving differential cross sections for ω^0 and η^0 production and a determination of the ω^0 density-matrix elements. Results on the higher regions of 3π mass can be found elsewhere.[1-3] A detailed discussion of the entire $pp\pi^+\pi^-\pi^0$ channel can be found in the work of Benson.[4] We define the "spectator" proton (p_s) to be the slower of the two protons in the bubble chamber. All of our events have both protons visible, which limits p_s to have momentum greater than ~60 MeV/c.

Differential cross sections. – Figure 1 (unshaded) shows a histogram of the 3π invariant mass in the ω^0 and η^0 regions and indicates a fairly small background under the peaks. We restrict our further attention to the ω^0 (720-860 MeV/c^2) and η^0 (530-570 MeV/c^2) mass regions.

Differential cross sections for the forward region (small $-t$) are shown in Fig. 2(a). We have plotted the data against the variable $t' = t - t_{\min}$ in order to compensate for the slight smearing of the data (due to Fermi momentum of the target neutron) that occurs in a straight t plot. t' is calculated for each event by transforming the beam into the outgoing 3π-p c.m.-system frame. Typical values of $t_{\min}$ in the ω^0 region are from 0.01 to 0.1 BeV^2.

In order to relate our observed forward cross sections to those on a free neutron, $\pi^+n \to p\pi^+\pi^-\pi^0$, one must account for the reduction due to the Pauli exclusion principle when the production is on a neutron in the deuteron.[4-6] This effect is pronounced only in the region $-t < 0.1$ BeV^2 and we show such a correction in the first t' bin of the ω^0 differential cross section [Fig. 2(a)]. The size of the correction depends on the t-dependent ratio of spin-flip to spin-nonflip cross sections off free neutrons, on the choice of the deuteron form factor, and on the minimum spectator momentum visible in our chamber (~60 MeV/c), but in any case is fairly insignificant for our data. The correction we show is for a pure spin-flip free-neutron cross section.

There is some evidence for a forward dip in the η^0 cross section and perhaps for some leveling off in the ω^0 cross section. We have examined the behavior for small t' for masses other than the ω^0 and η^0. There is no evidence for a sudden change in slopes at these masses and in fact,

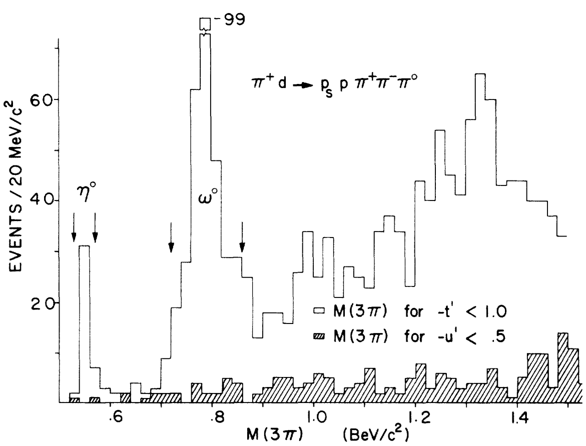

FIG. 1. Unshaded: invariant mass of $\pi^+\pi^-\pi^0$ for events with $-t' < 1.0$ BeV^2. Shaded: invariant mass of $\pi^+\pi^-\pi^0$ for events with $-u' < 0.5$ BeV^2. The regions of ω^0 and η^0 selection for Fig. 2 are indicated by the arrows. The definitions of t' and u' can be found in the text.

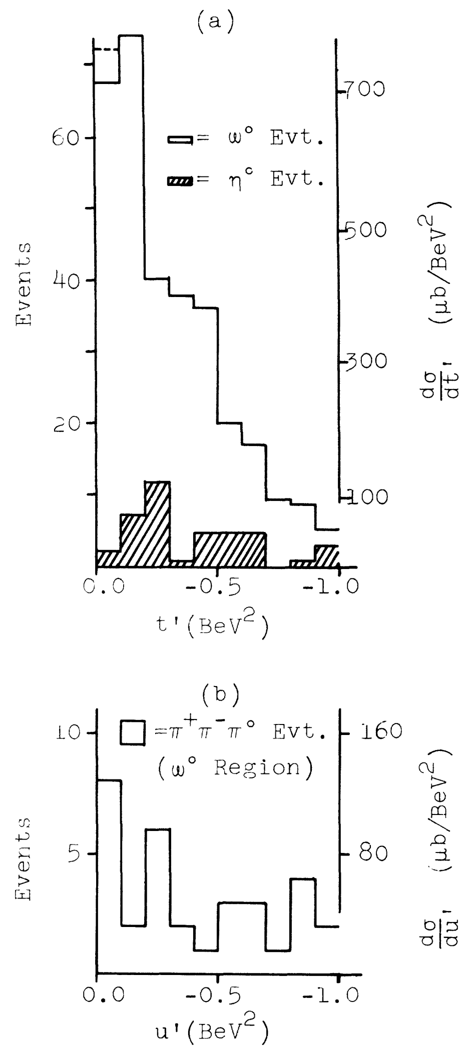

FIG. 2. (a) Unshaded: differential cross section for $\pi^+d \to p_s p + (\omega^0 \to \pi^+\pi^-\pi^0)$. The dotted line in the first bin shows correction to approximate the production on a free neutron. Shaded: differential cross section for $\pi^+d \to p_s p + (\eta^0 \to \pi^+\pi^-\pi^0$ or $\pi^+\pi^-\gamma)$. (b) Differential cross section for $\pi^+\pi^-\pi^0$ production near the backward direction and in the ω^0 mass region. See text and Fig. 1 (shaded). All cross sections have been corrected for undetected events with invisible spectator protons.

within our statistics, the behavior at small t' varies smoothly throughout the entire mass region from 500 to 2200 MeV/c^2. All traces of a forward dip vanish above the ω^0 region but reappear in the region 1250-1400 MeV/c^2. At masses above 1400 MeV/c^2 the cross sections fall off somewhat more slowly with t' and tend to flatten out above $-t' \sim 0.6$.

The behavior of the differential cross section near the backward direction is shown in Fig. 2(b), where we indicate the distribution of events in the ω^0 mass region versus $u' = u - u_{\min}$. (A typical value of $u_{\min}$ for these events is +0.02 BeV^2.) There appears to be a small backward peaking which, in fact, persists for the regions of higher 3π mass (not shown). In contrast to the forward region, the backward cross section $d^2\sigma/dMdu'$ shows only a smooth dependence on $M(3\pi)$. In other words, a plot of $M(3\pi)$ for various u' slices in the region $0 < -u' < 0.5$ BeV^2 shows no evidence of an ω^0 (or any other) peak above background (see Fig. 1). There is, however, some evidence of an ω^0 enhancement in the 3π mass spectrum for the region $0.5 < -u' < 1.0$ BeV^2 (not shown). We are limited by statistics from investigating this backward behavior in any more detail.

Density matrix of the omega. —We proceed to calculate the density-matrix elements $\rho_{mm'}$ which describe the omega spin. The angular distribution of the normal to the omega decay plane (defined as $\hat{\pi}^- \times \hat{\pi}^+$ in the omega c.m. frame) is given by[7]

$$\frac{d^2W}{d\Omega} = \frac{3}{8\pi}\{[2\rho_{00}\cos^2\theta + (1-\rho_{00})\sin^2\theta] - 2\sqrt{2}\,\mathrm{Re}\rho_{10} \times \sin2\theta\cos\varphi - 2\rho_{1\,-1}\sin^2\theta\cos2\varphi\}. \quad (1)$$

We define our coordinate system according to Gottfried and Jackson.[8] The z axis is along the beam in the c.m. frame of the omega. The y axis is given by (beam direction)$\times\hat{\omega}$ in the lab (note $\hat{y} \to -\hat{y}$ has the same effect as $\mathrm{Re}\rho_{10} \to -\mathrm{Re}\rho_{10}$). The x axis is $\hat{x} = \hat{y}\times\hat{z}$. The Fermi motion of the struck neutron in the reaction $\pi^+d \to \omega^0 pp_s$ gives rise to an uncertainty as to how to calculate $\hat{y}$. In the spirit of the impulse approximation one should perhaps use the direction $\hat{y}'$ = (beam direction) $\times\hat{\omega}$ in the c.m. frame of the outgoing ω-p system. With this $\hat{y}'$ the angle θ' is the same as θ above but φ' varies from φ by about ±5° on the average, due to the small spectator momentum. This uncertainty is negligible, compared with our errors, in our determination of $\mathrm{Re}\rho_{10}$ and $\rho_{1\,-1}$.

To determine ρ_{00} and $\rho_{1\,-1}$ we integrate (1) alternately over φ and θ to get

$$dW/d(\cos\theta) = \tfrac{3}{4}[2\rho_{00}\cos^2\theta + (1-\rho_{00})\sin^2\theta], \quad (2)$$

$$\frac{dW}{d\varphi} = \frac{1}{2\pi}[1 - 2\rho_{1\,-1}\cos2\varphi]. \quad (3)$$

These angular distributions, along with curves corresponding to the best-fit values of $\rho_{00} = 0.40 \pm 0.04$ and $\rho_{1\,-1} = 0.15 \pm 0.04$, are shown in Figs. 3(a) and 3(b). The data were folded about $\cos\theta = 0$ and $\varphi = 180°$ before fitting.

In order to determine $\mathrm{Re}\rho_{10}$ we first fold the distribution (1) about $\varphi = 180°$ to get $d^2W'/d\Omega = 2d^2W/d\Omega$. We then perform a subtraction:

$$\frac{d^2W''}{d\Omega} \equiv \left[\frac{d^2W'}{d\Omega}(\theta,\varphi) - \frac{d^2W'}{d\Omega}(\pi-\theta,\varphi)\right] = -\frac{3\sqrt{2}}{\pi}\mathrm{Re}\rho_{10}\sin2\theta\cos\varphi, \quad (4)$$

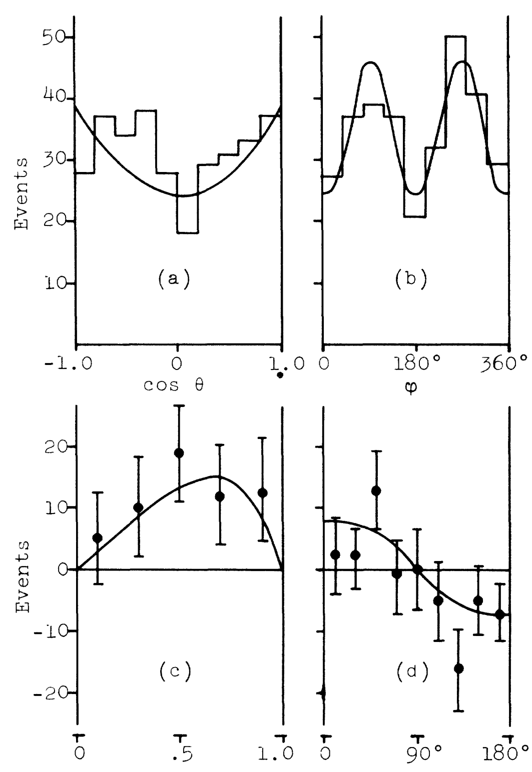

FIG. 3. Angular distributions of decay-plane normal for 313 events in the ω^0 mass region and with $-t < 1.0$ BeV^2. (a) Events versus $\cos\theta$ with best-fit curve from Eq. (2) giving $\rho_{00} = 0.40 \pm 0.04$. (b) Events versus φ with best-fit curve from Eq. (3) giving $\rho_{1\,-1} = 0.15 \pm 0.04$. (c) Subtracted distribution versus $\cos\theta$ with best-fit curve from Eq. (7) giving $\mathrm{Re}\rho_{10} = -0.097 \pm 0.030$. (d) Subtracted distribution versus φ with best-fit curve from Eq. (5) giving $\mathrm{Re}\rho_{10} = -0.070 \pm 0.024$.

where $0 \leq \cos\theta \leq 1$ and $0 \leq \varphi \leq 180°$. This gives, on integrating over θ,

$$\frac{dW''}{d\varphi} = \frac{-2\sqrt{2}}{\pi} \mathrm{Re}\rho_{10} \cos\varphi. \tag{5}$$

This $dW''/d\varphi$ distribution is shown in Fig. 3(d) along with the best fit curve which has $\mathrm{Re}\rho_{10} = -0.070 \pm 0.024$. To check this with the $\cos\theta$ distribution we define

$$\frac{d^2W'''}{d\Omega} \equiv \left[\frac{d^2W''}{d\Omega}(\theta,\varphi) - \frac{d^2W''}{d\Omega}(\theta, \pi-\varphi)\right] = \frac{-6\sqrt{2}}{\pi} \mathrm{Re}\rho_{10} \sin 2\theta \cos\varphi, \tag{6}$$

where $0 \leq \cos\theta \leq 1$, $0 \leq \varphi \leq 90°$ now.

We can integrate this over φ to get

$$\frac{dW'''}{d(\cos\theta)} = \frac{-6\sqrt{2}}{\pi} \mathrm{Re}\rho_{10} \sin 2\theta. \tag{7}$$

The distribution (7) is shown in Fig. 3(c) along with the best-fit curve, which has $\mathrm{Re}\rho_{10} = -0.097 \pm 0.030$.

We have also determined $\mathrm{Re}\rho_{10}$ by taking the average value of $\sin 2\theta \cos\varphi$ over the data (i.e., over the distribution $dW'/d\Omega$). This procedure gives

$$\mathrm{Re}\rho_{10} = \frac{-5}{4\sqrt{2}} \langle \sin 2\theta \cos\varphi \rangle = -0.08 \pm 0.03. \tag{8}$$

The corresponding value of $\mathrm{Re}\rho_{10}$ for the mass region just above the omega is -0.03 ± 0.03. Therefore we make no correction for the small background under the omega peak. Thus all three methods give consistent results for $\mathrm{Re}\rho_{10}$.

In summary, the values of the omega density matrix elements from this experiment are:

$$\rho_{00} = 0.40 \pm 0.04,$$

$$\rho_{1\,-1} = 0.15 \pm 0.04,$$

$$\mathrm{Re}\rho_{10} = -0.08 \pm 0.025$$

[average value for $-t(\mathrm{beam} \to \omega) \leq 1.0\ \mathrm{BeV}^2$]. One should interpret these values as being heavily weighted towards low $-t$, since the $-t$ distribution [Fig. 2(a)] is strongly peaked towards low values.

We have also calculated the rho values as a function of $-t$ (in the case of $\mathrm{Re}\rho_{10}$, using the averaging method only) and these results can be found in Henyey, Kajantie, and Kane.[9] Other published results on the reaction $\pi^+ d \to pp\omega^0$ are presented in Alitti et al.[10]

It seems evident from the appearance of Figs. 3(c) and 3(d) that our results support a small negative value for $\mathrm{Re}\rho_{10}$. [Note that a positive value of $\mathrm{Re}\rho_{10}$ flips the curves of Figs. 3(c) and 3(d) about the abscissa.] A negative value for $\mathrm{Re}\rho_{10}$ is in disagreement with various theoretical models, as has been pointed out in Ref. 9.

We are grateful to the staff at Brookhaven National Laboratory for their competent help in obtaining the exposure.

---

*Work supported in part by the U. S. Atomic Energy Commission.

†Deceased.

[1]G. Benson et al., Phys. Rev. Letters 12, 600 (1964).

[2]G. Benson et al., Phys. Rev. Letters 16, 1177 (1966).

[3]G. Benson et al., Phys. Rev. Letters 17, 1234 (1966).

[4]G. C. Benson, thesis, University of Michigan, 1966 (obtainable from University Microfilms, Ann Arbor, Mich.)

[5]I. Butterworth et al., Phys. Rev. Letters 15, 734 (1965).

[6]V. Stenger et al., Phys. Rev. 134, B1111 (1964).

[7]J. D. Jackson, Nuovo Cimento 34, 1644 (1964).

[8]K. Gottfried and J. D. Jackson, Nuovo Cimento 33, 309 (1964).

[9]F. Henyey, K. Kajantie, and G. L. Kane, Phys. Rev. Letters 21, 1782 (1968).

[10]J. Alitti et al., Phys. Letters 21, 354 (1966), present a tabulation of results on $\pi^+ d \to pp\omega^0$ at 1.7 and 3.25 BeV/c, and also on $\pi N \to \omega^0 N^*$ at various momenta.